

Vortex Lattice Melting in 2D Superconductors and Josephson Arrays

M. Franz and S. Teitel

Department of Physics and Astronomy, University of Rochester, Rochester, New York 14627

(Received 18 March 1994; revised manuscript received 22 April 1994)

Simulations of 2D vortex lattice melting in superconducting films are performed in the London limit. A detailed finite size scaling test of the theory of dislocation mediated melting in 2D indicates a weakly first order transition, and no hexatic liquid phase. However, the shear modulus vanishes discontinuously at melting, with a value in good agreement with this theory.

PACS numbers: 74.60.Ge, 64.60.-i, 74.50.+r, 74.76.-w

Interest in the melting of two dimensional (2D) vortex lattices has revived recently due to the belief that the strongly fluctuating, layered, high- T_c superconductors may behave 2D-like in sufficiently large magnetic fields [1]. This 2D melting transition has generally been believed to be described by the Kosterlitz-Thouless-Nelson-Halperin-Young (KTNHY) theory [2-4] of dislocation mediated melting. However, the very existence of a 2D vortex lattice at any finite T has been recently questioned by Moore [5]. High order, high T perturbative expansions [6] similarly show no evidence for freezing into a vortex lattice in 2D. Several Monte Carlo (MC) simulations [7], however, find clear evidence for melting at a finite T_m . Hu and MacDonald [7] find this transition to be first order, in opposition to the KTNHY theory.

The above cited simulations have all been performed in the "lowest Landau level" approximation, in which the complex order parameter $\psi(\mathbf{r})$ is expanded in the eigenstates of the Gaussian part of the Landau-Ginzburg free-energy functional. Alternatively, one may use the London approximation, in which $|\psi(\mathbf{r})|$ is assumed constant and only the phase of ψ fluctuates. In this limit, the problem can be efficiently simulated via the well known mapping [8] onto the 2D Coulomb gas. Logarithmically interacting point charges model vortices in the phase of $\psi(\mathbf{r})$. For a uniform magnetic field B , one has a fixed density B/Φ_0 of positive integer charges on a uniform neutralizing background (Φ_0 is the flux quantum). The London approximation should be valid whenever the bare vortex core radius $\xi_0 \ll a_v$, the average spacing between vortices. This corresponds to temperatures well below the mean field transition temperature, where vortex lattice melting is expected to occur. Earlier simulations of this 2D Coulomb gas [9] show evidence for a finite T_m and suggest that melting is weakly first order. Here we report on new simulations in this London approximation, in which we carry out the first finite size scaling analysis of the melting transition, making a detailed comparison with the KTNHY theory. We show that the shear modulus jumps discontinuously to zero at T_m with a value very close to the KTNHY prediction; however, we find no evidence for a hexatic liquid phase. We test the order of the melting transition by using the histogram method, and find that it is weakly first order, consistent with earlier suggestions.

The model we simulate is given by the Hamiltonian

$$\mathcal{H} = \frac{1}{2} \sum_{ij} (n_i - f)(n_j - f)V(\mathbf{r}_i - \mathbf{r}_j), \quad (1)$$

where we have discretized the continuum to the sites i of a periodic triangular grid with spacing a_0 and length La_0 . $n_i = 0$, or $+1$, is the point charge (vorticity) at site i . The neutralizing background charge is $f = (\sqrt{3}a_0^2/2)(B/\Phi_0) = (a_0/a_v)^2$, and $V(\mathbf{r})$ is the lattice Coulomb potential in 2D, which solves

$$\Delta^2 V(\mathbf{r}) = -2\pi\delta_{\mathbf{r},0} \quad (2)$$

subject to periodic boundary conditions. Δ^2 is the discrete Laplacian. To keep the total energy finite, one must require charge neutrality, i.e., the number of point charges $N_c \equiv \sum_i n_i = Nf$, where $N = L^2$. Thus f is the density of point charges. Further details may be found in Ref. [10]. We always choose f commensurate with L , so that the ground state will be a perfect triangular charge (vortex) lattice. The connection between Eq. (1) and a superconductor is obtained by measuring the Coulomb gas temperature in units of $\Phi_0^2 d/8\pi^2 \lambda^2$, where λ is the magnetic penetration length and d the film thickness [3,8].

We study charge densities $f = 1/m^2$, with $m = 3$ to 12, and fixed $N_c \approx 100$. Detailed finite size scaling analysis is done for the specific case of $f = 1/49$ and $N_c = 16, 25, \dots, 169$. Our MC updating scheme is as follows. A charge is selected at random and moved to a site within a radius $\sim a_v/2$. This excitation is then accepted or rejected using the standard Metropolis algorithm. We call N_c such attempts one MC sweep. At low T , we also make global moves by attempting to shift entire rows of charges by one space. Such shearing excitations help to accelerate equilibration near melting. Data are collected by heating from the ground state. At each T we discard 30 000 MC sweeps to equilibrate. Then, starting from this equilibrated configuration, we perform 4-6 independent runs of 100 000 sweeps each to compute averages. Errors are estimated from the standard deviation of these independent runs. To verify the consistency of our results, we have also cooled from a random configuration; no substantial hysteresis is found.

The physical quantities we measure are as follows: (i)

The inverse dielectric function,

$$\epsilon^{-1}(T) \equiv \lim_{\mathbf{k} \rightarrow 0} \left\{ 1 - \frac{2\pi}{k^2 T N} \langle n_{\mathbf{k}} n_{-\mathbf{k}} \rangle \right\}, \quad (3)$$

where $n_{\mathbf{k}} = \sum_i n_i \exp(-i\mathbf{k} \cdot \mathbf{r}_i)$. The vanishing of ϵ^{-1} upon heating signals an “insulator-conductor” transition in the Coulomb gas. As ϵ^{-1} can be mapped onto the helicity modulus of the superconductor [11], its vanishing signals the loss of superconducting phase coherence. We approximate the $\mathbf{k} \rightarrow 0$ limit by averaging ϵ^{-1} over the three smallest wave vectors. (ii) The sixfold orientational order correlation,

$$\varphi_6(T) \equiv \frac{1}{N_c^2} \sum_{ij} \langle e^{i6(\theta_i - \theta_j)} \rangle, \quad (4)$$

where the sum is only over sites with charges $n_i = +1$, and θ_i is the angle of the bond from n_i to its nearest neighbor, relative to a fixed direction. (iii) The structure function,

$$S(\mathbf{k}) \equiv \frac{1}{N_c} \langle n_{\mathbf{k}} n_{-\mathbf{k}} \rangle = \frac{1}{N_c} \sum_{ij} e^{i\mathbf{k} \cdot (\mathbf{r}_i - \mathbf{r}_j)} \langle n_i n_j \rangle. \quad (5)$$

In Fig. 1, we plot $\epsilon^{-1}(T)$ and $\varphi_6(T)$, versus T , for $f = 1/49$ and $N_c = 169$. The behavior of $\varphi_6(T)$ indicates two separate transitions at $T_c(f)$ and T_m . For a simple visualization of the resulting three phases, we show in Fig. 2 intensity plots of $S(\mathbf{k})$, for \mathbf{k} 's in the first Brillouin zone (BZ). We show results for three different values of T , with the data for each T restricted to one-third of the BZ. For $T = 0.003$ [Fig. 2(a)], just below $T_c(f)$, we see a regular array of sharp Bragg peaks, indicating long range translational order. Thus for $T < T_c(f)$, the vortex lattice is pinned to the discretizing grid. For $T = 0.0065$ [Fig. 2(b)], just below T_m , we see a regular array of peaks, but the peaks now have finite width consistent with the power law singularities characteristic of the algebraic translational order expected for a 2D lattice in the continuum. Thus for $T_c(f) < T < T_m$, we have a “floating” vortex lattice which is depinned from the grid.

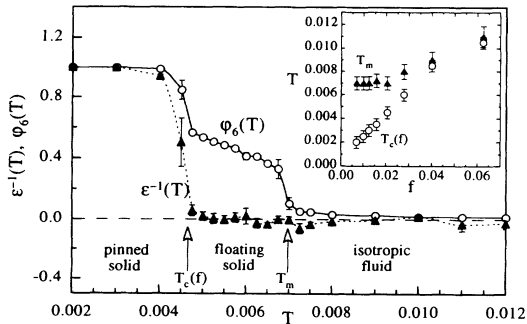


FIG. 1. Inverse dielectric function $\epsilon^{-1}(T)$ and orientational correlation $\varphi_6(T)$ versus T for $f = 1/49$, $N_c = 169$. Inset shows the dependence of the transitions T_c and T_m on charge density f . Solid and dashed lines are guides to the eye only.

For $T = 0.0075$ [Fig. 2(c)], slightly above T_m , we see a rotationally invariant structure ($\varphi_6 \sim 0$), typical for a liquid.

Returning to Fig. 1, we see that ϵ^{-1} vanishes at the depinning transition $T_c(f)$; the floating lattice has lost superconducting phase coherence. This just reflects the flux flow resistance to be expected from an unpinned vortex lattice, which is free to drift transversely to an applied dc current. Our results explicitly show that the absence of phase coherence in this $\mathbf{k} \rightarrow 0$ sense does not imply the absence of a well defined vortex lattice.

In the inset to Fig. 1, we show the dependence of $T_c(f)$ and T_m on the charge density f . Only for sufficiently dilute systems, $f < 1/25$, is there a floating lattice phase; for $f > 1/25$ there is a single transition from a pinned lattice to a liquid. As f decreases, $T_c(f) \sim f \rightarrow 0$, while T_m quickly approaches a finite constant $T_m = 0.0070 \pm 0.0005$, in good agreement with the melting temperature found in earlier continuum simulations [9]. In terms of the superconductor, this means a vortex lattice melting at $T_m = 0.0070 \Phi_0^2 d / 8\pi^2 \lambda^2$, well within the bounds estimated by Fisher [3] from the KTNHY theory.

The transition at $T_c(f)$ is an artifact of our discretizing the continuum; the limit of a uniform film is given by $f \rightarrow 0$, and, since $T_c(f \rightarrow 0) \rightarrow 0$, the pinned phase disappears. However, for the related problem of a periodic superconducting network such as a Josephson junction array [12], our discretization of space in Eq. (1) represents the discrete physical structure of the network. f is the number of vortices per unit cell of the network, and the sites i in Eq. (1) are those of the dual lattice of the periodic network. In this case $T_c(f)$ represents a physical depinning transition. For $T < T_c(f)$, the vor-

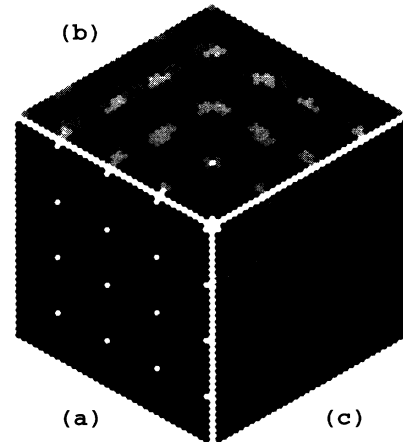


FIG. 2. Structure function $S(\mathbf{k})$ in the first Brillouin zone (BZ) for $f = 1/49$, $N_c = 63$, for three values of T . Data for each T are restricted to one third of the BZ. (a) $T = 0.003$, just below T_c , in the “pinned lattice” state. (b) $T = 0.0065$, just below T_m , in the “floating lattice” state. (c) $T = 0.0075$, just above T_m , in the liquid. Intensities are plotted nonlinearly to enhance features.

tex lattice is pinned to the periodic network and a true superconducting state exists. For $T_c(f) < T < T_m$, the vortex lattice is depinned; any applied dc current, no matter how small, will result in a finite linear "flux flow" resistivity. Our result that $T_c(f) \rightarrow 0$ as $f \rightarrow 0$ is consistent with early commensurability arguments for arrays by Teitel and Jayaprakash [13].

To investigate the nature of the melting transition T_m , we consider in detail the case $f = 1/49$, for which T_m is well separated from T_c . Our approach is guided by the KTNHY theory [2]. For a 2D lattice in the continuum, translational correlations decay algebraically with a temperature dependent exponent, $\langle e^{i\mathbf{G}\cdot(\mathbf{r}_i - \mathbf{r}_j)} \rangle \sim |\mathbf{r}_i - \mathbf{r}_j|^{-\eta_{\mathbf{G}}(T)}$, where \mathbf{G} is a reciprocal lattice vector of the real space charge lattice. For a 2D superconductor, where the vortex compressibility is infinite, $\eta_{\mathbf{G}}(T) = k_B T |\mathbf{G}|^2 / 4\pi\mu$, where μ is the vortex shear modulus. If \mathbf{G}_1 is the shortest reciprocal lattice vector, then the KTNHY theory predicts that at T_m , $\eta_{\mathbf{G}_1}$ takes a discontinuous jump to infinity from the universal value of $\eta_{\mathbf{G}_1}(T_m^-) = 1/3$.

To test this prediction, we measure the height of peaks in $S(\mathbf{k})$. From Eq. (5), these scale as

$$S(\mathbf{G}) \sim L^{2-\eta_{\mathbf{G}}(T)} \text{ for } T < T_m. \quad (6)$$

Above T_m , translational order has exponential decay with a correlation length ξ . One then obtains

$$S(\mathbf{G}) \sim \xi^2 \text{ for } T > T_m. \quad (7)$$

In Fig. 3(a) we plot $S(\mathbf{G}_1)/L^2$ versus L on a log-log

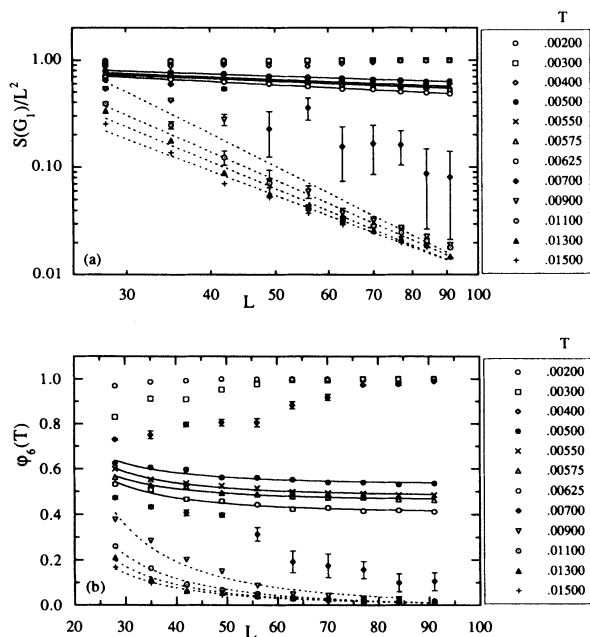


FIG. 3. (a) Finite size scaling of $S(\mathbf{G}_1)/L^2$ (note the log-log scale). Solid and dashed lines are fits by Eq. (6). (b) Finite size scaling of $\varphi_6(T)$. Solid and dashed lines are fits by Eq. (8).

scale, for several different T . The data fall on straight lines, confirming the expected power-law behavior. These straight lines fall into three distinct groups. For $T < T_c \simeq 0.0045$, $S(\mathbf{G}_1)/L^2 \sim 1$, indicating the long range order of the pinned lattice. For $T_c < T < T_m \simeq 0.007$, we find algebraic decay, $S(\mathbf{G}_1)/L^2 \sim L^{-\eta_{\mathbf{G}}(T)}$. For $T > T_m$, we find $S(\mathbf{G}_1)/L^2 \sim L^{-x}$, with $x \rightarrow 2$ as T increases, consistent with the short range order of a liquid. The lines in Fig. 3(a) are a fit by Eq. (6); the resulting exponents $\eta_{\mathbf{G}_1}(T)$ are shown in Table I. We see that $\eta_{\mathbf{G}_1}$ first exceeds the KTNHY universal value of $1/3$ at $T = 0.0065$, very close to our estimated $T_m \simeq 0.007$, where the slopes of the lines in Fig. 3(a) show an apparent discontinuous jump. Similar results have very recently been obtained within the lowest Landau level approximation [14].

As a consistency check, we have also computed $S(\mathbf{G}_2)$, where $\mathbf{G}_2 = 2\mathbf{G}_1$. Using similar fits as in Fig. 3(a), we show our results for $\eta_{\mathbf{G}_2}$ in Table I. We see that $\eta_{\mathbf{G}_2} \simeq 4\eta_{\mathbf{G}_1}$ as expected, since $\eta_{\mathbf{G}} \sim |\mathbf{G}|^2$.

We now consider the orientational order. Below T_m , KTNHY predict long range sixfold orientational order given by $\langle e^{i6(\theta(r) - \theta(0))} \rangle \sim \alpha e^{-r/\xi_6} + \varphi_6^\infty$. For $\xi_6 \ll L$, one obtains from Eq. (4)

$$\varphi_6 \sim 2\pi\alpha \left(\frac{\xi_6}{L} \right)^2 + \varphi_6^\infty. \quad (8)$$

Above T_m , KTNHY predict a hexatic liquid phase, with algebraic orientational order $\langle e^{i6(\theta(r) - \theta(0))} \rangle \sim r^{-\eta_6(T)}$ with $\eta_6(T) < 1/4$. In such a case, one would have

$$\varphi_6 \sim L^{-\eta_6}. \quad (9)$$

At higher T , KTNHY predict an isotropic liquid, with short ranged orientational order. In this case, Eq. (8) again holds, but with $\varphi_6^\infty = 0$ [15]. In Fig. 3(b) we display $\varphi_6(T)$ versus L for various T . In the floating solid below T_m we find that $\varphi_6(T)$ saturates to a finite value as L increases, indicating long range order. Solid lines represent a least square fits to Eq. (8), and the extracted values of φ_6^∞ are shown in Table I. Above T_m , we try fits to both Eqs. (8) and (9); we find that Eq. (8) always

TABLE I. Temperature dependence of $\eta_{\mathbf{G}_1}(T)$, $\eta_{\mathbf{G}_2}(T)$, and φ_6^∞ [see Eqs. (6) and (8)].

T	$\eta_{\mathbf{G}_1}(T)$	$\eta_{\mathbf{G}_2}(T)$	φ_6^∞
0.00475	0.188 ± 0.008	0.704 ± 0.055	0.571 ± 0.007
0.00500	0.207 ± 0.007	0.806 ± 0.032	0.529 ± 0.005
0.00525	0.211 ± 0.007	0.852 ± 0.028	0.504 ± 0.004
0.00550	0.248 ± 0.005	0.998 ± 0.019	0.476 ± 0.003
0.00575	0.255 ± 0.008	0.999 ± 0.029	0.458 ± 0.003
0.00600	0.296 ± 0.006	1.065 ± 0.028	0.426 ± 0.007
0.00625	0.319 ± 0.010	1.191 ± 0.016	0.403 ± 0.004
0.00650	0.4 ± 0.16	1.4 ± 0.22	0.33 ± 0.030
0.00675	1.4 ± 0.31	2.0 ± 0.31	0.20 ± 0.041
0.00750	3.4 ± 0.37	3.4 ± 0.44	0.03 ± 0.046
0.01100	2.8 ± 0.23	2.9 ± 0.30	-0.01 ± 0.032
0.01500	2.2 ± 0.12	2.1 ± 0.22	0.00 ± 0.020

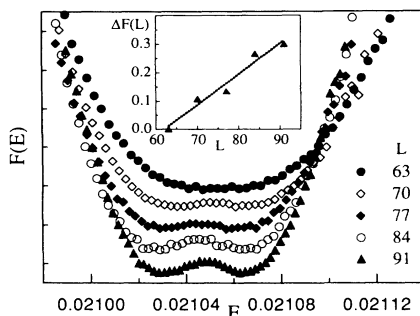


FIG. 4. Free energy $F(E)$ versus E , at T_m , for several sizes L . The growth in energy barrier ΔF with increasing L (see inset) indicates a first order transition. Curves for different L are offset from each other for clarity.

gives the superior fit, with $\varphi_6^\infty \simeq 0$. Thus we find no evidence for a hexatic liquid above T_m .

The absence of the hexatic liquid suggests that the melting transition may not be of the KTNHY type, but is perhaps weakly first order as found by Hu and MacDonald [7], and as suggested in Ref. [9]. To examine this possibility, we measured the energy distribution $P(E) \sim e^{-F(E)/T}$ at T_m [16], and in Fig. 4 we plot the resulting free energy $F(E)$ versus E . We see a double well structure with an energy barrier ΔF between two coexisting phases. In the inset to Fig. 4 we show ΔF versus L . The growth in ΔF as L increases signals a first order transition, although our sizes remain too small and our data too noisy, to see clearly the predicted scaling $\Delta F \sim L$. To determine the distributions in Fig. 4, we have computed $P(E)$ at fixed $T \simeq T_m$, and then extrapolated [17] to determine $P(E)$ at nearby T , finding the precise value of T that gives equal minima in $F(E)$. In this way we obtain an improved estimate $T_m \simeq 0.0066$.

To conclude, our results clearly establish the melting of the 2D vortex lattice, within the London approximation, at a finite T_m . This transition is first order, with melting directly into an isotropic vortex liquid; no hexatic liquid is found. The first order transition, however, is very weak, so that the jump in η_G at melting (and hence in the vortex shear modulus μ) remains very close to the KTNHY universal prediction.

We are grateful to T. Chen, D. A. Huse, D. R. Nelson, and Z. Tešanović for useful discussions. This work was supported by DOE Grant No. DE-FG02-89ER14017. One of us (M.F.) acknowledges the Rush Rhees Fellow-

ship of the University of Rochester for additional support.

- [1] D. S. Fisher, M. P. A. Fisher, and D. A. Huse, Phys. Rev. B **43**, 130 (1991); L. I. Glazman and A. E. Koshelev, Phys. Rev. B **43**, 2835 (1991).
- [2] J. M. Kosterlitz and D. J. Thouless, J. Phys. C **6**, 1181 (1973); D. R. Nelson and B. I. Halperin, Phys. Rev. B **19**, 2457 (1979); A. P. Young, Phys. Rev. B **19**, 1855 (1979).
- [3] D. S. Fisher, Phys. Rev. B **22**, 1190 (1980).
- [4] S. Doniach and B. Huberman, Phys. Rev. Lett. **42**, 1169 (1979).
- [5] M. A. Moore, Phys. Rev. B **45**, 7336 (1992); J. A. O'Neill and M. A. Moore, Phys. Rev. Lett. **69**, 2582 (1992); Phys. Rev. B **48**, 374 (1993).
- [6] E. Brézin, A. Fujita, and S. Hikami, Phys. Rev. Lett. **65**, 1949 (1990); S. Hikami, A. Fujita, and A. I. Larkin, Phys. Rev. B **44**, 10400 (1991).
- [7] Z. Tešanović and L. Xing, Phys. Rev. Lett. **67**, 2729 (1991); Y. Kato and N. Nagaosa, Phys. Rev. B **47**, 2932 (1993); Jun Hu and A. H. MacDonald, Phys. Rev. Lett. **71**, 432 (1993).
- [8] P. Minnhagen, Phys. Rev. B **23**, 5745 (1981).
- [9] Ph. Choquard and J. Clerouin, Phys. Rev. Lett. **50**, 2086 (1983); J. M. Caillol, D. Levesque, J. J. Weis, and J. P. Hansen, J. Stat. Phys. **28**, 325 (1982).
- [10] J.-R. Lee and S. Teitel, Phys. Rev. B **46**, 3247 (1992).
- [11] P. Minnhagen and G. G. Warren, Phys. Rev. B **24**, 2526 (1981); T. Ohta and D. Jasnow, Phys. Rev. B **20**, 130 (1979).
- [12] For a review, see *Proceedings of the NATO Advanced Research Workshop on Coherence in Superconducting Networks, Delft, 1987*, edited by J. E. Mooij and G. B. J. Schön [Physica (Amsterdam) **142B**, 1-302 (1988)].
- [13] S. Teitel and C. Jayaprakash, Phys. Rev. Lett. **51**, 1999 (1983).
- [14] R. Šašik and D. Stroud, Ohio State University report, 1994 (to be published).
- [15] In principle, the discretizing mesh acts like an ordering field for sixfold orientational order, and so even in the isotropic liquid one might find φ_6^∞ small but finite. Our numerical result that $\varphi_6^\infty \simeq 0$ above T_m indicates that this is a very small effect at the small f which we are studying.
- [16] J. Lee and J. M. Kosterlitz, Phys. Rev. Lett. **65**, 137 (1990).
- [17] A. M. Ferrenberg and R. H. Swendsen, Phys. Rev. Lett. **61**, 2635 (1988).

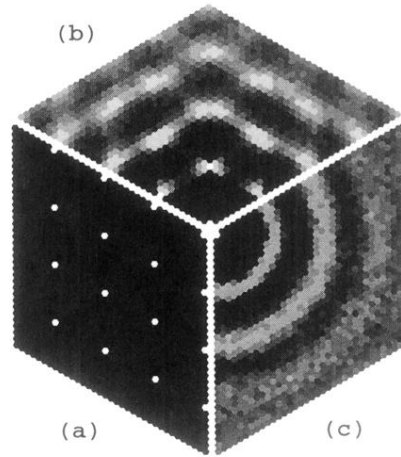


FIG. 2. Structure function $S(\mathbf{k})$ in the first Brillouin zone (BZ) for $f = 1/49$, $N_c = 63$, for three values of T . Data for each T are restricted to one third of the BZ. (a) $T = 0.003$, just below T_c , in the “pinned lattice” state. (b) $T = 0.0065$, just below T_m , in the “floating lattice” state. (c) $T = 0.0075$, just above T_m , in the liquid. Intensities are plotted nonlinearly to enhance features.